*Inorg. Chem.* **2009**, *48*, 671−680


# Tunneling Barrier Effects on Photoinduced Charge Transfer through Covalent Rigid Rod-Like Bridges

**David Hanss and Oliver S. Wenger***

*Department of Inorganic, Analytical and Applied Chemistry, University of Geneva, 30 Quai Ernest-Ansermet, CH-1211 Geneva 4, Switzerland*

Received September 26, 2008

Four homologous dyads with a phenothiazine donor, rigid variable-length *p*-xylene bridges, and a ruthenium(II) tris(2,2′-bipyridine) acceptor were synthesized. Photoexcitation of these donor-bridge-acceptor molecules in the presence of excess methylviologen generates a highly oxidizing Ru(III) intermediate, which triggers an intramolecular phenothiazine-to-ruthenium(III) electron transfer that is mediated by the oligo-*p*-xylene spacers. The rates for this process were determined using transient absorption spectroscopy, and they are found to decrease exponentially with increasing donor−acceptor distance. This decrease occurs with an attenuation factor $\beta$ of 0.77 Å$^{-1}$ and is substantially stronger than for analogous donor-bridge-acceptor molecules where the acceptor is a rhenium(I) tricarbonyl diimine complex ($\beta = 0.52$ Å$^{-1}$). This striking finding is interpreted in terms of a larger barrier to hole tunneling in the ruthenium dyads relative to the rhenium systems.

## Introduction

Photoinduced electron transfer is a key process in natural photosynthesis and has therefore received much attention in the context of artificial light-to-chemical energy conversion.[1−8] Marcus' prediction of a Gaussian free energy dependence of electron transfer rates has stimulated a wealth of experimental work on donor−acceptor systems.[9,10] First direct experimental evidence for the predicted behavior, namely a decrease of reaction rates for systems in which electron transfer is highly exergonic, appeared more than 20 years ago.[11,12] Since then, numerous studies have reported on this so-called inverted driving force effect, and there exist now many artificial donor−acceptor systems that exploit this phenomenon for the kinetic stabilization of charge-separated states.[13−18] Under favorable conditions, the energy that is stored transitorily in such long-lived charge-separated states can be used to drive other chemical reactions that are thermodynamically uphill.[19]

An intriguing question is whether biological photosynthesis is based on long-lived charge-separated states that are stabilized exclusively by the above mentioned driving force effects or whether electronic coupling effects also play an essential role. The electronic coupling between a donor and an acceptor, often abbreviated as $H_{DA}$, is a measure for the (bridge-mediated) orbital overlap between the two redox

* To whom correspondence should be addressed. E-mail: oliver.wenger@unige.ch.

(1) Balzani, V. *Electron transfer in chemistry*; VCH Wiley: Weinheim, 2001; Vol. *3*.
(2) Wasielewski, M. R. *Chem. Rev.* **1992**, *92*, 435–461.
(3) Gust, D.; Moore, T. A.; Moore, A. L. *Acc. Chem. Res.* **2001**, *34*, 40–48.
(4) Gray, H. B.; Winkler, J. R. *Annu. Rev. Biochem.* **1996**, *65*, 537–561.
(5) De Cola, L.; Belser, P. *Coord. Chem. Rev.* **1998**, *177*, 301–346.
(6) Balzani, V.; Juris, A. *Coord. Chem. Rev.* **2001**, *211*, 97–115.
(7) Guldi, D. M. *Chem. Soc. Rev.* **2002**, *31*, 22–36.
(8) Flamigni, L.; Barigelletti, F.; Armaroli, N.; Collin, J.-P.; Dixon, I. M.; Sauvage, J.-P.; Williams, J. A. G. *Coord. Chem. Rev.* **1999**, *192*, 671–682.
(9) Marcus, R. A.; Sutin, N. *Biochim. Biophys. Acta* **1985**, *811*, 265–322.
(10) Marcus, R. A. *Annu. Rev. Phys. Chem.* **1964**, *15*, 155–196.
(11) Miller, J. R.; Calcaterra, L. T.; Closs, G. L. *J. Am. Chem. Soc.* **1984**, *106*, 3047–3049.
(12) Closs, G. L.; Miller, J. R. *Science* **1988**, *240*, 440–447.
(13) Fox, L. S.; Kozik, M.; Winkler, J. R.; Gray, H. B. *Science* **1990**, *247*, 1069–1071.
(14) Imahori, H.; Tamaki, K.; Guldi, D. M.; Luo, C. P.; Fujitsuka, M.; Ito, O.; Sakata, Y.; Fukuzumi, S. *J. Am. Chem. Soc.* **2001**, *123*, 2607–2617.
(15) Kodis, G.; Liddell, P. A.; de la Garza, L.; Moore, A. L.; Moore, T. A.; Gust, D. *J. Mater. Chem.* **2002**, *12*, 2100–2108.
(16) Flamigni, L.; Baranoff, E.; Collin, J.-P.; Sauvage, J.-P. *Chem.−Eur. J.* **2006**, *12*, 6592–6606.
(17) Borgström, M.; Shaikh, N.; Johansson, O.; Anderlund, M. F.; Styring, S.; Åkermark, B.; Magnuson, A.; Hammarström, L. *J. Am. Chem. Soc.* **2005**, *127*, 17504–17515.
(18) Lopez, R.; Leiva, A. M.; Zuloaga, F.; Loeb, B.; Norambuena, E.; Omberg, K. M.; Schoonover, J. R.; Striplin, D.; Devenney, M.; Meyer, T. J. *Inorg. Chem.* **1999**, *38*, 2924–2930.
(19) Steinberg-Yfrach, G.; Liddell, P. A.; Hung, S. C.; Moore, A. L.; Gust, D.; Moore, T. A. *Nature* **1997**, *385*, 239–241.

10.1021/ic801841k CCC: $40.75 © 2009 American Chemical Society
Published on Web 12/10/2008

partners and is known to have an important influence on electron transfer rates.[20] The key point here is that $H_{DA}$ for an energy-storing charge-separation and an energy-wasting charge-recombination reaction may differ,[21] whereby an additional kinetic stabilization of the energy-rich charge-separated state may result. This is a comparatively poorly investigated aspect of photoinduced electron transfer. In proteins, as well as in artificial systems with distant redox partners, electron transfers were found to depend crucially on the intervening medium between the donor and the acceptor.[20−25] Depending on the chemical nature of the bridging molecules between the two reactants, electron transfer rates may be strongly or weakly distance dependent. In systems where the transferring electron can thermodynamically access the energy levels of the bridge, long-range electron transfer exhibits a particularly shallow distance dependence because the electron can "hop" from one bridging unit to the next. Many molecular wires, typically highly $\pi$-conjugated molecules, function on the basis of this hopping mechanism.[26−29] For systems with large donor-bridge energy gaps, a more strongly distance dependent tunneling mechanism takes over;[20−25] this is typically the case for proteins, alkanes, and even oligo-*p*-phenylene bridges. In this process, an electron tunnels through the barrier imposed by the bridging medium separating the donor from the acceptor, and their electronic coupling $H_{DA}$ is expected to be a function of the tunneling barrier height.[30−32] If the barrier to photoinduced charge-separation is significantly smaller than that associated with thermal charge-recombination, this should result in differential electronic coupling that favors the energy-storing over the energy-wasting process. In other words, a long-lived charge-separated state may be the result.

The electronic donor−acceptor coupling $H_{DA}$ in (weakly coupled) long-range electron transfer systems is not a parameter that is readily accessible from simple experiments. Prior work has demonstrated that electronic coupling effects can be studied by investigating the distance dependence of electron tunneling rates in a series of homologous donor-bridge-acceptor molecules.[20−30] This has prompted us to synthesize and investigate a series of four dyads composed of a ruthenium(II) tris-2,2′-bipyridine ($Ru(bpy)_3^{2+}$) complex, variable-length oligo-*p*-xylene bridges, and a phenothiazine (PTZ) moiety as shown in Scheme 1. In these systems, intramolecular charge transfer from the phenothiazine to a photogenerated $Ru(bpy)_3^{3+}$ species likely occurs primarily via a hole tunneling process. Through comparison of the distance dependence for hole tunneling through the xylene bridges in these ruthenium dyads with that previously observed by us in analogous rhenium-xylene-phenothiazine dyads,[33] it is possible to explore tunneling barrier effects for charge transfer across oligo-*p*-xylene bridges.

**Scheme 1.** Four Donor-Bridge-Acceptor Molecules Synthesized and Investigated in This Work

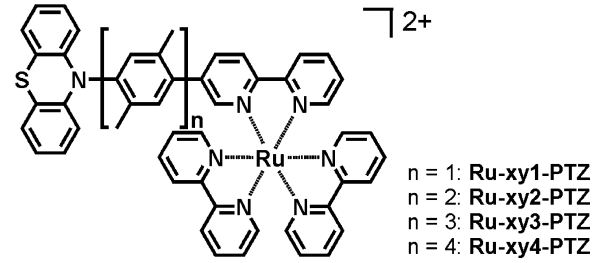


## Results and Discussion

**Synthesis.** The synthesis of the donor-bridge-acceptor molecules from Scheme 1 is based on the ligand synthesis outlined in Scheme 2. For the shortest member of the dyad series, phenothiazine (**1**) is coupled to a trimethylsilyl (TMS) protected bromo-*p*-xylene molecule (**2**) using a very efficient palladium(0) catalyzed N−C coupling reaction.[33,34] This reaction is so efficient that when unprotected 2,5-dibromo-1,4-dimethylbenzene is used as a coupling partner, only the doubly N−C coupled reaction product is obtained, regardless of the phenothiazine/xylene reaction stoichiometry. A TMS/halogen exchange reaction on molecule **3** yields a product (**4**) that can be coupled to 5-(tri-*n*-butyltin)-2,2′-bipyridine (**5**);[33,35] the latter was synthesized in two steps following previously published protocols.[36,37] The syntheses of the longer members of the dyad series begin with the same N−C coupling as above, but in these cases the reaction partner is a bi-*p*-xylene molecule (**7**) that is accessible from commercially available chemicals in three reaction steps.[33] The synthesis of this precursor is straightforward, but its purification by column chromatography is tedious. The phenothiazine-bixylene coupling product (**8**) is deprotected with ICl in essentially quantitative yields, thereby allowing the gram-scale isolation of intermediate **9**. This molecule may either be coupled to 5-(tri-*n*-butyltin)-2,2′-bipyridine **5** or the *p*-xylene bridge may be further elongated by reacting it with

(20) Gray, H. B.; Winkler, J. R. *Proc. Natl. Acad. Sci. U.S.A.* **2005**, *102*, 3534–3539.
(21) Wiberg, J.; Guo, L. J.; Pettersson, K.; Nilsson, D.; Ljungdahl, T.; Mårtensson, J.; Albinsson, B. *J. Am. Chem. Soc.* **2007**, *129*, 155–163.
(22) Winkler, J. R.; Gray, H. B. *J. Biol. Inorg. Chem.* **1997**, *2*, 399–404.
(23) Wenger, O. S.; Leigh, B. S.; Villahermosa, R. M.; Gray, H. B.; Winkler, J. R. *Science* **2005**, *307*, 99–102.
(24) Wenger, O. S.; Gray, H. B.; Winkler, J. R. *Chimia* **2005**, *59*, 94–96.
(25) Kilså, K.; Kajanus, J.; Macpherson, A. N.; Mårtensson, J.; Albinsson, B. *J. Am. Chem. Soc.* **2001**, *123*, 3069–3080.
(26) Davis, W. B.; Svec, W. A.; Ratner, M. A.; Wasielewski, M. R. *Nature* **1998**, *396*, 60–63.
(27) Fortage, J.; Goransson, E.; Blart, E.; Becker, H. C.; Hammarström, L.; Odobel, F. *Chem. Commun.* **2007**, 4629–4631.
(28) Giacalone, F.; Segura, J. L.; Martin, N.; Guldi, D. M. *J. Am. Chem. Soc.* **2004**, *126*, 5340–5341.
(29) Winters, M. U.; Dahlstedt, E.; Blades, H. E.; Wilson, C. J.; Frampton, M. J.; Anderson, H. L.; Albinsson, B. *J. Am. Chem. Soc.* **2007**, *129*, 4291–4297.
(30) Pettersson, K.; Wiberg, J.; Ljungdahl, T.; Mårtensson, J.; Albinsson, B. *J. Phys. Chem. A* **2006**, *110*, 319–326.
(31) McConnell, H. M. *J. Chem. Phys.* **1961**, *35*, 508–515.
(32) Nitzan, A.; Jortner, J.; Wilkie, J.; Burin, A. L.; Ratner, M. A. *J. Phys. Chem. B* **2000**, *104*, 5661–5665.
(33) Hanss, D.; Wenger, O. S. *Inorg. Chem.* **2008**, *47*, 9081–9084.
(34) Okamoto, T.; Kuratsu, M.; Kozaki, M.; Hirotsu, K.; Ichimura, A.; Matsushita, T.; Okada, K. *Org. Lett.* **2004**, *6*, 3493–3496.
(35) Hensel, V.; Schlüter, A. D. *Liebigs Ann.* **1997**, 303–309.
(36) Brotschi, C.; Mathis, G.; Leumann, C. J. *Chem.−Eur. J.* **2005**, *11*, 1911–1923.
(37) Haino, T.; Araki, H.; Yamanaka, Y.; Fukazawa, Y. *Tetrahedron Lett.* **2001**, *42*, 3203–3206.

**Scheme 2.** Syntheses of the Donor-Bridge Ligands[a]

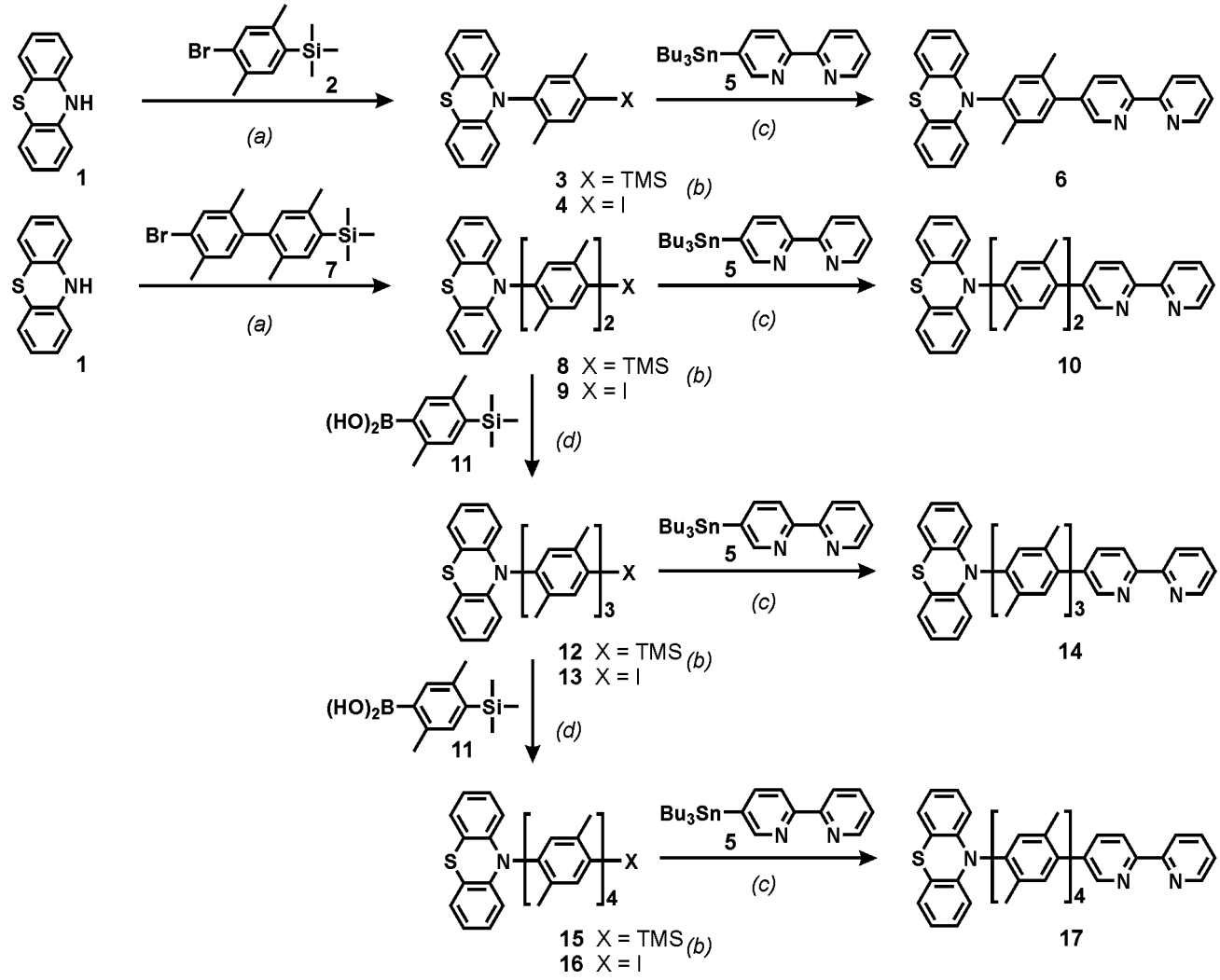


[a] (a) $Pd(dba)_2$, P(*t*.-Bu)$_3$, *t*.-BuOK, toluene (60°C); (b) ICl, $CH_3CN/CH_2Cl_2$ 3:1 (25°C); (c) $Pd(PPh_3)_4$, *m*-xylene (reflux); (d) $Pd(PPh_3)_4$, $Na_2CO_3$, toluene/ethanol/water 85:10:5 (reflux).

the asymmetric building block **11** in a Suzuki cross-coupling reaction.[38,39] In the latter case one obtains the TMS-protected phenothiazine-tri-*p*-xylene molecule **12** that must again be activated subsequently by TMS/halogen exchange with iodine monochloride. The resulting molecule **13** resembles intermediate **9** in that it can be either reacted with bipyridine **5** or elongated with boronic acid **11**. In principle, this modular synthetic scheme could be pursued ad infinitum, but as the spectroscopic work will show, it is not meaningful to synthesize molecules with more than four *p*-xylene bridging units for the present study. The number of reaction steps necessary for the synthesis of the four dyads in Scheme 1 (including the final complexation of the phenothiazine-xylene-bipyridine ligands from Scheme 2 to $Ru(bpy)_2Cl_2$,[40] but not counting the steps needed for synthesis of the building blocks **2**, **5**, **7**, and **11**) are as follows: 4 for Ru-xy$_1$-PTZ, 4 for Ru-xy$_2$-PTZ, 6 for Ru-xy$_3$-PTZ, and 8 for Ru-xy$_4$-PTZ.

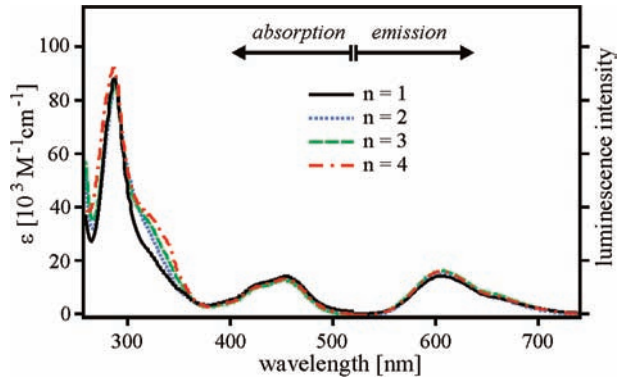


**Figure 1.** Optical absorption and luminescence spectra of the four Ru-xy$_n$-PTZ dyads from Scheme 1 in acetonitrile solution at room temperature.

**Optical Spectroscopy and Electrochemistry.** Figure 1 shows the optical absorption and luminescence spectra of the four ruthenium dyads from Scheme 1 in acetonitrile solution. The solid black line represents data obtained for the mono-*p*-xylene bridged molecule Ru-xy$_1$-PTZ. By analogy to previously published data on the $Ru(bpy)_3^{2+}$ com-

(38) Walther, M. E.; Wenger, O. S. *Dalton Trans.* **2008**, 6311−6318.
(39) Durola, F.; Sauvage, J.-P.; Wenger, O. S. *Chem. Commun.* **2006**, 171–173.
(40) Sullivan, B. P.; Salmon, D. J.; Meyer, T. J. *Inorg. Chem.* **1978**, *17*, 3334–3341.

**Table 1.** Donor-Acceptor Distances $r_{DA}$, MLCT Excited State Lifetimes $\tau_{MLCT}$, and Redox Potentials of the Ru-xy$_n$-PTZ Dyads and Two Reference Molecules

| | $r_{DA}$ [Å][a] | $\tau_{MLCT}$ [ns][b] | $E(Ru(bpy)_3^{2+/+})$[c] | $E(Ru(bpy)_3^{3+/2+})$[c] | $E(PTZ^{+/0})$[c] |
|---|---|---|---|---|---|
| Ru-xy$_1$-PTZ | 10.6 | 842 | −1.22 | 1.22 | 0.79 |
| Ru-xy$_2$-PTZ | 14.9 | 828 | −1.22 | 1.26 | 0.75 |
| Ru-xy$_3$-PTZ | 19.2 | 861 | −1.17 | 1.21 | 0.80 |
| Ru-xy$_4$-PTZ | 23.5 | 855 | −1.27 | 1.17 | 0.73 |
| $Ru(bpy)_3^{2+}$ | | 865 | −1.28 | 1.26 | |
| 10-methyl-PTZ | | | | | 0.79[d] |

[a] Measured from the Ru(II) ion to the phenothiazine-N. [b] Measured in freeze−pump−thaw deoxygenated acetonitrile solution at room temperature. [c] Measured using an Ag/AgCl quasi-reference electrode in acetonitrile, but reported versus SCE. [d] From reference 48.

plex,[41] the intense absorption at 290 nm is assigned to a bpy-localized $\pi$-$\pi$* transition, and the weaker band centered around 450 nm must be due to Ru(II) → bpy metal to ligand charge transfer (MLCT). The luminescence (on the right) is assigned to the reverse MLCT transition, but originating from a state with triplet spin multiplicity. Indeed the Ru-xy$_1$-PTZ and the $Ru(bpy)_3^{2+}$ absorption and luminescence spectra are virtually identical; the phenothiazine and xylene absorptions occur at shorter wavelengths, and the presence of these molecular moieties does not affect the MLCT emission spectrum of the ruthenium complex.

Interestingly, all these statements also apply to the longer dyads. The four absorption spectra are very nearly identical; the only significant difference between them is a slightly increasing extinction around 325 nm with increasing oligo-*p*-xylene bridge length, manifesting itself in the appearance of a shoulder to the intense bpy $\pi$-$\pi$* band. This behavior is in strong contrast to that commonly observed for oligo-*p*-phenylene spacers: For unsubstituted phenyl bridges very pronounced red-shifts (>50 nm) of the UV absorption bands are usually observed upon elongation;[33,42−44] the same is true for oligo-fluorene bridges.[45,46] The absence of increasing $\pi$-conjugation with increasing bridge length in our oligo-*p*-xylene bridges indicates that the equilibrium dihedral angle between two neighboring *p*-xylene units must be substantially greater than between two unsubstituted phenyls. This is attributed to a steric effect. The luminescence spectra of the four dyads are also nearly identical; neither the luminescence band shape nor its intensity is affected by the presence of the phenothiazine and the xylene bridging units. Time-resolved luminescence spectroscopy reveals that the metal-to-ligand charge-transfer (MLCT) excited-state dynamics, too, are indistinguishable from those of the $Ru(bpy)_3^{2+}$ parent complex. As seen from Table 1, excited-state lifetimes ($\tau_{MLCT}$) scattering around 850 ns in deoxygenated (room temperature) acetonitrile solution were obtained for the four dyads. For comparison, the MLCT lifetime of the $Ru(bpy)_3^{2+}$ reference complex, determined under identical experimental conditions, is 865 ns. The observation of identical luminescence properties among the Ru-xy$_n$-PTZ and $Ru(bpy)_3^{2+}$ molecules is somewhat surprising because another study has reported on reductive quenching of the $Ru(bpy)_3^{2+}$ MLCT excited state by a covalently attached phenothiazine electron donor.[47] To shed more light on this issue, we performed cyclic voltammetry experiments on our donor-bridge-acceptor molecules. The electrochemical results are summarized in Table 1: Three reversible one-electron waves are observed, notably a bpy → $bpy^-$ reduction at −1.22 V versus SCE, a Ru(II) → Ru(III) oxidation at 1.22 V versus SCE, and a phenothiazine oxidation at 0.77 V versus SCE. There are no discernible trends in the Ru-xy$_n$-PTZ series, and all potentials are very close to those of the reference molecules;[48] this is true for the $Ru(bpy)_3^{2+}$-based, as well as the PTZ-based, redox processes. One important conclusion from the electrochemical and spectroscopic results presented so far is that the Ru-xy$_n$-PTZ donor-bridge-acceptor molecules are weakly coupled systems in which the donors and acceptors exhibit mutually independent photophysical and electrochemical properties.

With the phenothiazine and ruthenium redox potentials at hand, one may now also attempt to understand the absence of the above mentioned luminescence quenching by electron transfer from phenothiazine to MLCT-excited ruthenium complexes: This MLCT state is 2.12 eV above the ground state, which sets the $Ru(bpy)_3^{2+/+}$ excited-state redox potential at a value of about 0.9 eV.[49] The thermodynamic driving force $\Delta G_{ET}$ for the charge-shift from phenothiazine to the excited $Ru(bpy)_3^{2+}$ complex can be calculated using the Weller equation which takes the dielectric constant of the solvent, as well as the average donor and acceptor radii, into account.[50−52] However, in first approximation it appears sufficient to estimate $\Delta G_{ET}$ as the difference between the $PTZ^{+/0}$ and $*Ru(bpy)_3^{2+/+}$ redox potentials, multiplied by the elemental charge. This yields $\Delta G_{ET} \approx -0.1$ eV, that is, PTZ → $*Ru(bpy)_3^{2+}$ electron transfer is only weakly exergonic. On the basis of the Ru MLCT excited-state decay constants $k_{MLCT}$ (which are the inverse of the MLCT luminescence lifetimes $\tau_{MLCT}$ reported in Table 1), we estimate that this excited-state electron transfer occurs with rate constants inferior to $10^5$ $s^{-1}$ in all four dyads. We attribute the slowness of this process to the above mentioned low reaction driving force. This interpretation is in line with a prior in-depth study of electron transfer between photoexcited $Ru(bpy)_3^{2+}$ and phenothiazine.[53]

**Bimolecular Flash-Quench Experiments.** With excited-state electron transfer being completely unobserved in our


(41) Caspar, J. V.; Meyer, T. J. *J. Am. Chem. Soc.* **1983**, *105*, 5583–5590.
(42) Weiss, E. A.; Ahrens, M. J.; Sinks, L. E.; Gusev, A. V.; Ratner, M. A.; Wasielewski, M. R. *J. Am. Chem. Soc.* **2004**, *126*, 5577–5584.
(43) Welter, S.; Lafolet, F.; Cecchetto, E.; Vergeer, F.; De Cola, L. *ChemPhysChem.* **2005**, *6*, 2417–2427.
(44) Indelli, M. T.; Chiorboli, C.; Flamigni, L.; De Cola, L.; Scandola, F. *Inorg. Chem.* **2007**, *46*, 5630–5641.
(45) Goldsmith, R. H.; Sinks, L. E.; Kelley, R. F.; Betzen, L. J.; Liu, W. H.; Weiss, E. A.; Ratner, M. A.; Wasielewski, M. R. *Proc. Natl. Acad. Sci. U.S.A.* **2005**, *102*, 3540–3545.
(46) Montes, V. A.; Perez-Bolivar, C.; Agarwal, N.; Shinar, J.; Anzenbacher, P. *J. Am. Chem. Soc.* **2006**, *128*, 12436–12438.
(47) Larson, S. L.; Elliott, C. M.; Kelley, D. F. *Inorg. Chem.* **1996**, *35*, 2070–2076.
(48) Chen, P. Y.; Westmoreland, T. D.; Danielson, E.; Schanze, K. S.; Anthon, D.; Neveux, P. E.; Meyer, T. J. *Inorg. Chem.* **1987**, *26*, 1116–1126.
(49) Roundhill, D. M. *Photochemistry and Photophysics of Metal Complexes*; Plenum Press: New York, 1994.
(50) Weller, A. *Z. Phys. Chem.* **1982**, *133*, 93–98.
(51) Rehm, D.; Weller, A. *Ber. Bunsen-Ges. Phys. Chem.* **1969**, *73*, 834.
(52) Marcus, R. A. *J. Chem. Phys.* **1965**, *43*, 679–701.

**Scheme 3.** Reaction Scheme and Timescales for Inter- and Intramolecular Electron Transfer Processes in the Ru-xy$_n$-PTZ Dyads in the Presence of Excess Methylviologen ($MV^{2+}$)

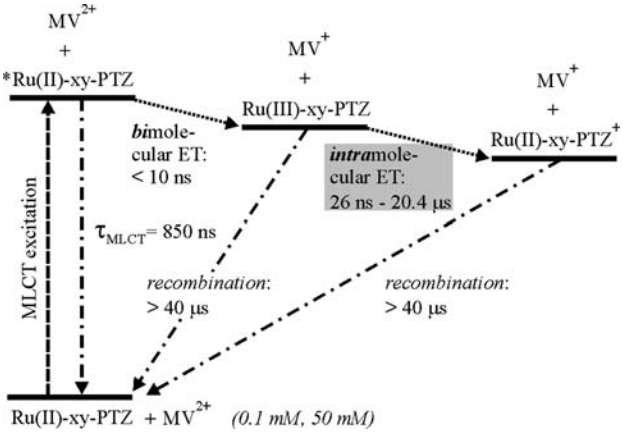


dyads, we turned to a flash-quench technique that uses excess methylviologen ($MV^{2+}$) as an external quencher as illustrated in Scheme 3.[54]

The Ru-xy$_n$-PTZ molecules, present at 0.1 mM concentrations, are photoexcited into the MLCT band at 532 or 457.9 nm (flash). The MLCT-excited Ru(II) is then oxidized by the methylviologen, present at 50 mM concentration, whereby a Ru(III) species and a methylviologen radical $MV^+$ are formed transitorily. This bimolecular MLCT quenching occurs within less than 10 ns since the rate constant for bimolecular *Ru(bpy)$_3^{2+}$ → $MV^{2+}$ electron transfer is nearly diffusion controlled with a value of $2.4 \times 10^9$ $M^{-1}$ $s^{-1}$.[49] The $MV^+$ radical has characteristic absorptions at ~400 nm and ~600 nm, and therefore the formation of this species can be monitored conveniently by transient absorption spectroscopy.[55] When the Ru(bpy)$_3^{2+}$ complex is oxidized, the Ru(II) → bpy MLCT absorption centered at 450 nm (Figure 1) disappears since the resulting Ru(III) species only has a very weak extinction coefficient at this wavelength; the result is a so-called bleach of the MLCT band in transient absorption experiments.[55]These features, an MLCT bleach at 450 nm due to the formation of Ru(III) and additional absorptions at ~400 nm and ~600 nm due to the formation of $MV^+$, are readily observed in the transient absorption spectra of Figure 2 (solid red line and dashed blue line).

The solid red trace was obtained on the Ru-xy$_3$-PTZ sample using a time gate that extends from immediately after the laser excitation pulse to 1 $\mu$s after the pulse. When this experiment is performed with the Ru(bpy)$_3^{2+}$ reference complex under identical conditions, the same transient spectrum results, and the positive signal at 400 nm and the negative signal at 450 nm both disappear on a >40 $\mu$s time scale. Indeed, in this case the disappearance of the $MV^+$ radical matches the reappearance of Ru(II), and one may

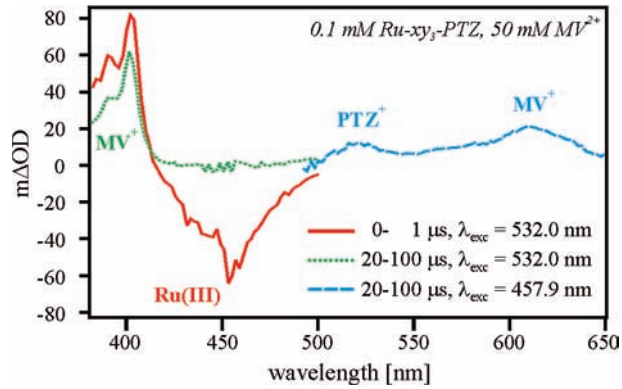


**Figure 2.** Transient absorption spectra measured on a deoxygenated 0.1 mM acetonitrile solution of the Ru-xy$_3$-PTZ dyad in the presence of 50 mM methylviologen ($MV^{2+}$) quencher using different time gates and excitation wavelengths ($\lambda_{exc}$).

thus conclude that bimolecular $MV^+$ → Ru(III) electron transfer is very slow, see the central dash-dotted downward arrow in Scheme 3. We now turn our attention back to the transient absorption data collected on the Ru-xy$_3$-PTZ dyad in Figure 2. The dotted green line is the transient absorption spectrum measured on the same sample using a time gate that starts 20 $\mu$s after the laser excitation pulse. We note that the $MV^+$ signal at ~400 nm is still present whereas the Ru(II) MLCT bleach at ~450 nm has disappeared completely. This is interpreted in terms of intramolecular PTZ → Ru(III) electron transfer: First, it is the only process that can lead to a recovery of the Ru(II) species on a time scale that is significantly shorter than that for bimolecular $MV^+$ → Ru(III) recombination. Second, in the transient absorption data from Figure 2 (dashed blue line), there is direct spectroscopic evidence for the $PTZ^{\bullet+}$ radical cation at ~520 nm. According to this interpretation, the dynamics of the Ru(II) recovery after bimolecular quenching with methylviologen should be different for Ru-xy$_n$-PTZ dyads with different oligo-*p*-xylene bridge lengths *n*. Indeed, this is the case as the MLCT bleach dynamics in Figure 3 demonstrate unambiguously. For these experiments, 0.1 mM solutions of the four dyads (abbreviated as xy1, xy2, xy3, xy4) and the Ru(bpy)$_3^{2+}$ reference complex (abbreviated as "ref") in freeze−pump−thaw deoxygenated acetonitrile were photoexcited with 10 ns, 532 nm laser pulses in presence of 50 mM methylviologen concentrations. Under these conditions, the MLCT bleach of the reference complex recovers marginally within the 10 $\mu$s time window of the upper panel of Figure 3 (orange trace). The Ru-xy$_4$-PTZ data (red trace) is substantially more recovered but far from being complete in 10 $\mu$s. The Ru-xy$_3$-PTZ data (green trace) on the other hand is perfectly resolved in this time window, whereas for the Ru-xy$_2$-PTZ dyad (blue trace) the MLCT bleach recovery appears to be almost instantaneous. When the bi-*p*-xylene bridged system is investigated on a shorter time scale, lower panel of Figure 3, it becomes nevertheless evident that its MLCT recovery is yet somewhat slower than that of the mono-*p*-xylene bridged dyad (purple trace). The important observation is that the shorter the bridge, the faster the Ru(II) MLCT recovery becomes. This makes perfect sense: The closer the PTZ donor and the photogenerated Ru(III) acceptor

(53) Borgström, M.; Johansson, O.; Lomoth, R.; Baudin, H. B.; Wallin, S.; Sun, L. C.; Åkermark, B.; Hammarström, L. *Inorg. Chem.* **2003**, *42*, 5173–5184.
(54) Bjerrum, M. J.; Casimiro, D. R.; Chang, I.-J.; Di Bilio, A. J.; Gray, H. B.; Hill, M. G.; Langen, R.; Mines, G. A.; Skov, L. K.; Winkler, J. R.; Wuttke, D. S. *J. Bioenerg. Biomembr.* **1995**, *27*, 295–302.
(55) Abrahamsson, M. L. A.; Baudin, H. B.; Tran, A.; Philouze, C.; Berg, K. E.; Raymond-Johansson, M. K.; Sun, L. C.; Åkermark, B.; Styring, S.; Hammarström, L. *Inorg. Chem.* **2002**, *41*, 1534–1544.

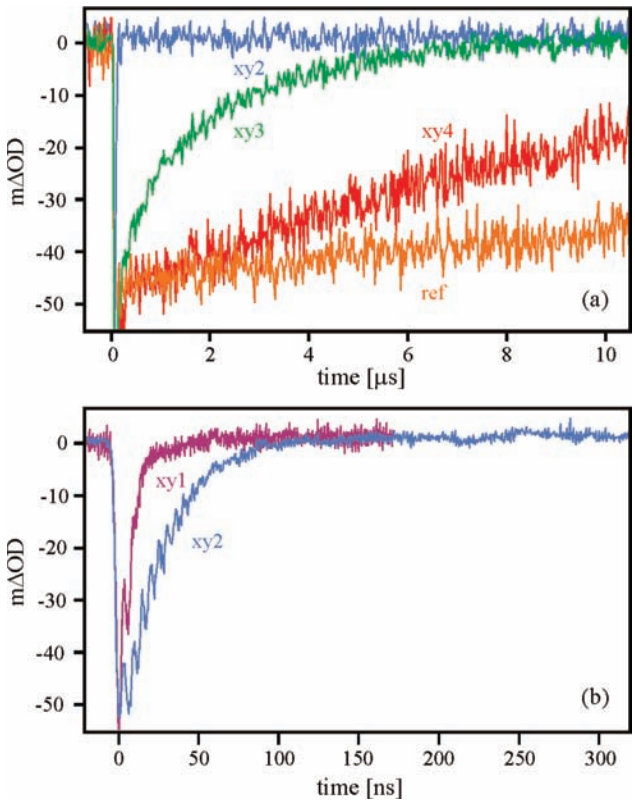


**Figure 3.** Recoveries of the Ru(II) → bpy MLCT absorption at 450 nm after pulsed (532 nm) excitation of deoxygenated (0.1 mM) acetonitrile solutions of the Ru-xy$_n$-PTZ dyads and a Ru(bpy)$_3^{2+}$ reference complex in presence of excess (50 mM) methylviologen.

are, the faster the intramolecular PTZ → Ru(III) electron transfer process will be. The MLCT recoveries for all four dyads are single exponential, but the Ru-xy$_1$-PTZ data is instrumentally limited. For the bi-, tri-, and tetra-*p*-xylene dyads it is possible to extract time constants for the Ru(II) formation via intramolecular electron transfer; the numerical values are 26 ns for Ru-xy$_2$-PTZ, 1.8 $\mu$s for Ru-xy$_3$-PTZ, and 20.4 $\mu$s for Ru-xy$_4$-PTZ.

The interpretation of the bridge-length dependent MLCT recoveries from Figure 3 in terms of intramolecular phenothiazine-to-ruthenium(III) electron transfer is corroborated by the time-resolved data displayed in Figure 4: The upper panel shows the MLCT recovery (at 450 nm) after photoexcitation of a 0.1 mM acetonitrile solution of the Ru-xy$_4$-PTZ dyad in presence of 50 mM methylviologen. The lower panel shows the temporal evolution of the transient absorption signal at 520 nm in the same sample. The 520 nm signal increases instantaneously at $t = 0$ because of absorption of reduced methylviologen ($MV^{\bullet+}$) at this wavelength.[55] This is followed by a much slower rise that must be due to $PTZ^{\bullet+}$ formation (see Figure 2). This rise is essentially identical to the MLCT recovery shown in the upper panel. In other words, the rate constant for $PTZ^{\bullet+}$ formation matches that for Ru(III) disappearance, which is conclusive evidence for phenothiazine-to-ruthenium(III) electron transfer.

In Figure 5, the natural logarithms of the PTZ → Ru(III) electron transfer rate constants $k_{ET}$ (extracted from the data in Figures 3 and 4) are plotted versus donor−acceptor distance as estimated (open circles). The three data points

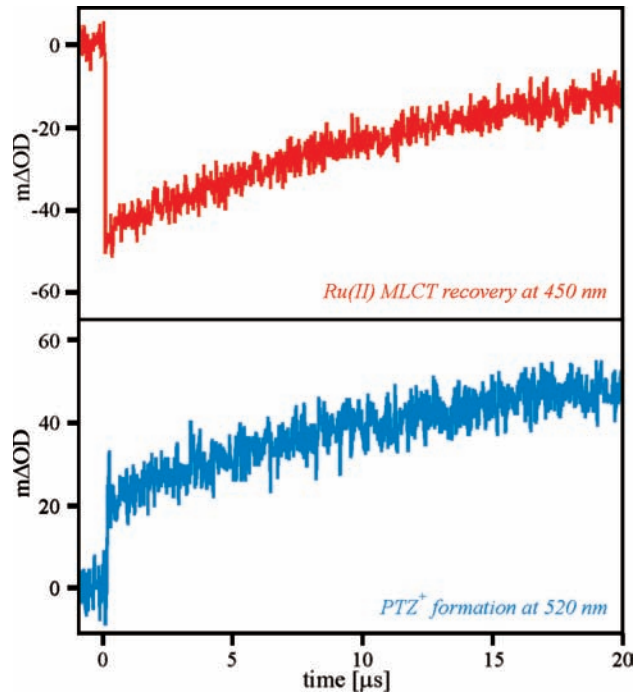


**Figure 4.** Temporal evolution of the transient absorption signals at 450 nm (upper panel, Ru(II) → bpy MLCT recovery) and 520 nm (lower panel, $PTZ^{\bullet+}$ formation) in a 0.1 mM deoxygenated acetonitrile solution of Ru-xy$_4$-PTZ in the presence of 50 mM methylviologen. The pump wavelength was 532.0 nm in both cases.

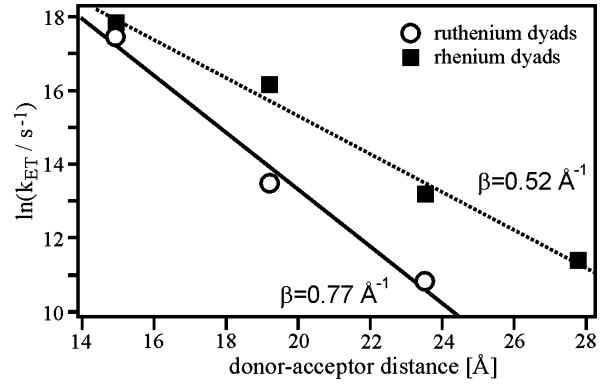


**Figure 5.** Plot of $\ln(k_{ET}/s^{-1})$ versus the donor−acceptor distance $r_{DA}$ for the Ru-xy$_n$-PTZ donor-bridge-acceptor molecules with $n = 2, 3, 4$ (open circles) and for analogous rhenium-xylene-phenothiazine dyads (filled squares).[33]

nearly fall onto a line, indicating that $k_{ET}$ decreases exponentially with increasing distance, which is typical behavior for a charge tunneling process.[20]

A linear regression fit to the Ru-xy$_n$-PTZ data in Figure 5 yields a slope of −0.77 Å$^{-1}$. The absolute value of this slope is the distance decay parameter $\beta$, and it contains information on the bridge-mediated electronic donor−acceptor coupling $H_{DA}$. A $\beta$-value of 0.77 Å$^{-1}$ is at the upper end of what has been previously observed for long-range electron transfer across covalent phenylene bridges: Prior studies on unsubstituted oligo-*p*-phenylene bridged dyads report on $\beta$-values ranging from 0.35 Å$^{-1}$ to 0.67 Å$^{-1}$.[42,44,56−58] A study on oligo-*p*-xylene mediated electron transfer found $\beta = 0.76$ Å$^{-1}$,[23,59] but the most striking observation is that in our prior study on phenothiazine-xylene-rhenium molecules, we found $\beta = 0.52$ Å$^{-1}$.[33] These rhenium donor-bridge-acceptor

**Scheme 4.** Redox Potentials of the Relevant Donor (PTZ), Bridge (4,4′-dimethyldiphenyl, dmdp), and Acceptor ($Ru(bpy)_3^{2+}$, $[Re(phen)(CO)_3(pyridine)]^+$) Moieties

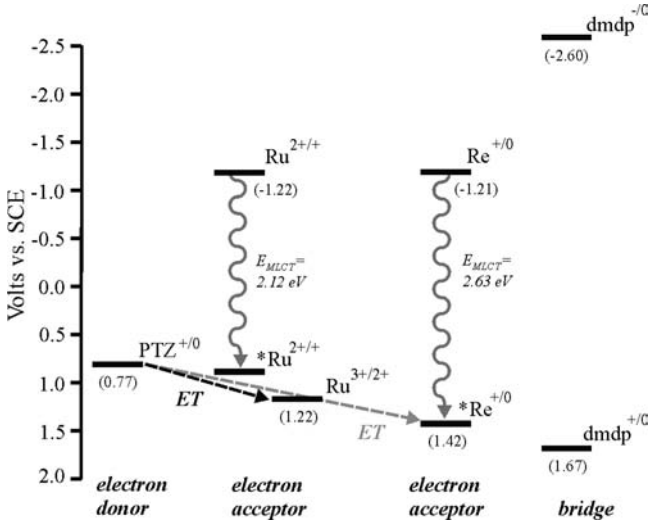


systems were structurally identical to the dyads investigated in the present study; the only difference is that the electron acceptor was a photoexcited rhenium(I) tricarbonyl 1,10-phenanthroline complex, $*[Re(phen)(CO)_3(pyridine)]^+$, instead of a photogenerated $Ru(bpy)_3^{3+}$ species. The data from our rhenium work has been included in Figure 5 (black squares and dotted line). From this comparison it is seen that long-range electron transfer is clearly less efficient in the newly investigated ruthenium systems. For instance, the 19.2 Å charge tunneling process across a tri-*p*-xylene bridge is more than an order of magnitude slower for the dyad with the ruthenium acceptor than for the system with the rhenium acceptor. Conversely, the 23.5 Å tunneling across a tetra-*p*-xylene bridge with the rhenium acceptor is almost equally fast as the 19.2 Å tunneling across a tri-*p*-xylene bridge with the ruthenium acceptor.

To understand where this difference in long-range electron transfer efficiencies comes from, it is necessary to consider the reaction energetics. Scheme 4 gives a graphical illustration of all relevant energy levels as estimated from the redox potentials of the PTZ electron donor, Ru and Re electron acceptors, and a dimethyldiphenyl (dmdp) molecule representing the bridge. This graph shows that the photoexcited Re complex is about 0.2 V more oxidizing than the $Ru(bpy)_3^{3+}$ complex.[33] The first conclusion we may draw is that PTZ → *Re electron transfer is more exergonic than PTZ → Ru(III) electron transfer. It has not been possible to measure the redox potentials of our oligo-*p*-xylene bridges; our best guess for their potentials therefore comes from a prior electrochemical study of the 4,4′-dimethyldiphenyl

**Scheme 5.** Energy Level Diagram for Hole Tunneling through Oligo-*p*-xylene Bridges with Photogenerated $Ru(bpy)_3^{3+}$ and Photoexcited $[Re(phen)(CO)_3(pyridine)]^+$ Hole Donors and Phenothiazine (PTZ) Hole Acceptors

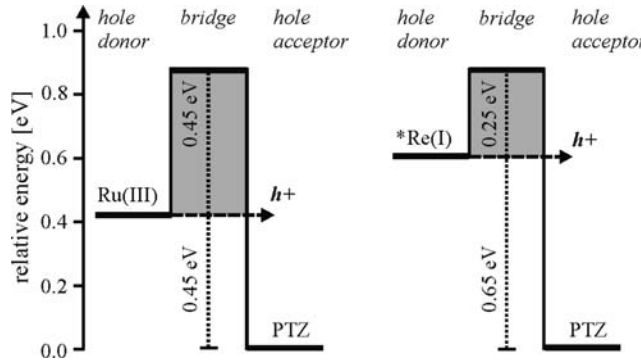


(dmdp) molecule.[60] The dmdp is oxidized at 1.67 V versus SCE and reduced at −2.60 V versus SCE; from this we conclude that the charge transfer in both the ruthenium and rhenium dyads occurs primarily via a *hole* tunneling rather than *electron* tunneling mechanism. The former mechanism involves a virtual one-electron *oxidation*, the latter a virtual one-electron *reduction* of the bridge. Because of the much closer energetic proximity of the one-electron oxidized bridge states relative to the donor and acceptor levels, a hole tunneling mechanism appears much more plausible than electron tunneling. It is therefore sensible to refer to the Ru and Re complexes as to hole donors, and the phenothiazine may be considered as a hole acceptor. This terminology is used in Scheme 5 in which we arbitrarily set the PTZ hole acceptor level to 0 eV. On the basis of the redox potentials and MLCT energies from Scheme 4, the bridge levels are ∼0.9 eV higher in energy, the Ru(III) level ∼0.45 eV, and the *Re(I) level ∼0.65 eV.

Even though this graph represents a very much simplified view and is semiquantitative at best, it illustrates two important things: (i) The driving force for charge transfer increases when replacing ruthenium by rhenium; (ii) the barrier to hole tunneling is greater in the ruthenium dyads than in the rhenium systems. Therein must lie the explanation for the different tunneling efficiencies (or different $\beta$-values) in the Ru-$xy_n$-PTZ and Re-$xy_n$-PTZ dyads: The probability $\kappa$ for a particle to tunnel through a square potential energy barrier is dependent on the mass ($m$) of the particle, the width of the barrier ($d$), and its height ($\Delta E$):[61]

$$\kappa \propto e^{-\frac{2}{\hbar}\sqrt{2 \cdot m \cdot \Delta E} \cdot d} \quad (1)$$

The barrier height dependence also shows up in superexchange theory for long-range electron transfer:[31] According to this model, the electronic donor−acceptor coupling $H_{DA}$ mediated by a bridge comprised of $n$ identical repeating units is a function of a barrier height called tunneling energy gap $\Delta\varepsilon$, the electronic coupling between the donor and the first bridging unit $h_{Db}$, the coupling between adjacent bridging units $h_{bb}$, and the electronic coupling between the last bridging unit and the acceptor $h_{bA}$:

(56) Helms, A.; Heiler, D.; McLendon, G. *J. Am. Chem. Soc.* **1992**, *114*, 6227–6238.
(57) Indelli, M. T.; Scandola, F.; Flamigni, L.; Collin, J.-P.; Sauvage, J.-P.; Sour, A. *Inorg. Chem.* **1997**, *36*, 4247–4250.
(58) Dance, Z. E. X.; Ahrens, M. J.; Vega, A. M.; Ricks, A. B.; McCamant, D. W.; Ratner, M. A.; Wasielewski, M. R. *J. Am. Chem. Soc.* **2008**, *130*, 830–832.
(59) Villahermosa, R. M. *Electron tunneling through phenylene bridges*; California Institute of Technology: Pasadena, CA, 2002.
(60) Ishiguro, K.; Nakano, T.; Shibata, H.; Sawaki, Y. *J. Am. Chem. Soc.* **1996**, *118*, 7255–7264.
(61) Gamov, G. *Z. Phys.* **1928**, *51*, 204–212.

$$H_{DA} = \frac{h_{Db}}{\Delta\varepsilon}\left(\frac{h_{bb}}{\Delta\varepsilon}\right)^{n-1} h_{bA} \quad (2)$$

The same superexchange model predicts that the distance decay constant $\beta$ is a function of only three parameters:

$$\beta = \frac{2}{\alpha}\ln\left(\frac{\Delta\varepsilon}{h_{bb}}\right) \quad (3)$$

where $\alpha$ is the length of the repeating bridge unit. Thus, the greater the barrier $\Delta\varepsilon$, the greater $\beta$ should be, which appears to be in line with our experimental observations (Figure 5 and Scheme 5). However, it is important to note that the barriers in Scheme 5 were estimated on the basis of redox potentials, that is, relaxed states, but the tunneling energy gap $\Delta\varepsilon$ in eqs 2 and 3 is a vertical energy gap at the transition state of the electron transfer process as illustrated in Scheme 6.

$\Delta\varepsilon$ is therefore a quantity that is not readily extracted from experiment, and the absolute values for $\Delta\varepsilon$ in the Ru-xy$_n$-PTZ and Re-xy$_n$-PTZ dyads cannot be determined. Furthermore, from Scheme 6 it also becomes evident that the magnitude of $\Delta\varepsilon$ is susceptible to driving force ($\Delta G_{ET}$) and reorganization energy ($\lambda$) variations. Since $\Delta G_{ET}$ changes between our Ru and Re dyads, this issue must be discussed briefly. Both the ruthenium and rhenium dyad series were investigated in the same solvent and in both cases the overall reaction is a charge shift. One might therefore expect relatively minor changes in $\lambda$ between the two series. Despite the ~0.2 eV driving force difference between them, quantification of the relative magnitude of $\Delta\varepsilon$ for the two systems remains elusive. It is possible, however, to estimate *effective* tunneling barriers $\Delta E_{eff}$ based on an expression that can be derived from eqs 1 and 3; these effective barriers are simply a function of the tunneling probability coefficient or $\beta$-value:[20,62]

$$\Delta E_{eff} = \left(\frac{\hbar^2}{8m_e}\right)\beta^2 \quad (4)$$

where $m_e$ is the mass of the electron, yielding a numerical value of 0.952 eV·Å$^2$ for the prefactor in eq 4. On the basis of this expression and the $\beta$ parameters determined above (0.77 Å$^{-1}$ and 0.52 Å$^{-1}$, respectively), one obtains $\Delta E_{eff}$ = 0.55 eV for the Ru-xy$_n$-PTZ systems and $\Delta E_{eff}$ = 0.26 eV for the Re-xy$_n$-PTZ dyads. These effective barriers are strikingly close to those estimated based on redox potentials (shaded areas in Scheme 5). While their close agreement may be a mere coincidence, this analysis nevertheless supports our interpretation of the different distance dependences in the Ru and Re dyads in terms of tunneling barrier changes, and it narrows the role played by the simultaneous driving force variation. The applicability of this analysis approach is supported by a very recent study that reports on a good correlation of distance decay parameters with tunneling barriers in a wide variety of different materials, ranging from semiconductors to proteins, water, and even vacuum.[62]

**Scheme 6.** Graphical Illustration of the Tunneling Energy Gap $\Delta\varepsilon$

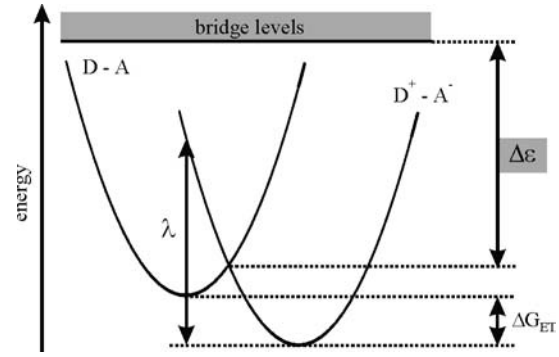


The observation of changing distance dependences for charge transfer across a given bridge for varying donor−acceptor couples is not without precedent. Recent experimental studies on DNA hairpins find $\beta$ values to depend strongly on the donor-bridge-acceptor energetics.[63,64] In particular, the hole tunneling efficiency across adenine bridging units was found to be a function of the tunneling energy gap: A 0.25 eV decrease in $\Delta\varepsilon$ lead to a decrease in $\beta$ from 1.1 Å$^{-1}$ to 0.71 Å$^{-1}$.[63,65] This experimentally observed tunneling energy effect was even more dramatic than the one calculated previously for hole transfer between vinyl groups separated by alkane bridges, where a 2.45 eV decrease in $\Delta\varepsilon$ reduced $\beta$ from 0.56 Å$^{-1}$ to 0.13 Å$^{-1}$.[66] Recent experimental work has shown that in a series of zinc and gold porphyrin dyads the rate of fixed-distance electron tunneling across different bridges with varying energies is inversely proportional to the donor-bridge energy gap $\Delta E_{Db}$.[25] More recent research relates this $\Delta E_{Db}$ dependence to the distance dependence for electron tunneling from a zinc(II) porphyrin to a gold(III) porphyrin via oligo-phenyleneethynylene (OPE) bridges and concludes that both the width (i. e., the donor−acceptor distance) and the height of the tunneling barrier ($\Delta E_{Db}$) determine long-range electron transfer rates across these bridges.[30] Computational work supports this conclusion.[67] Moreover, these calculations show that the distance dependence for electron transfer across OPE, oligo-phenylenevinylene (OPV), and other highly conjugated bridging molecules may be nonexponential and that this can be understood on the basis of decreasing donor-bridge energy gaps $\Delta E_{Db}$ with increasing bridge length.

Our oligo-*p*-xylene bridges represent an intermediate case between these strongly $\pi$-conjugated OPE and OPV bridges and the essentially nonconjugated adenine spacers in the DNA hairpins, which manifests itself in the magnitude of the distance decay parameters: For the OPV and OPE bridges, $\beta$ ranges from 0.03 Å$^{-1}$ to 0.39 Å$^{-1}$,[21,26,30,68] for

(62) Edwards, P. P.; Gray, H. B.; Lodge, M. T. J.; Williams, R. J. P. *Angew. Chem., Int. Ed.* **2008**, *47*, 6758–6765.
(63) Lewis, F. D.; Liu, J. Q.; Weigel, W.; Rettig, W.; Kurnikov, I. V.; Beratan, D. N. *Proc. Natl. Acad. Sci. U.S.A.* **2002**, *99*, 12536–12541.
(64) Tong, G. S. M.; Kurnikov, I. V.; Beratan, D. N. *J. Phys. Chem. B* **2002**, *106*, 2381–2392.
(65) Wenger, O. S. *Chimia* **2007**, *61*, 823–825.
(66) Paddon-Row, M. N.; Shephard, M. J.; Jordan, K. D. *J. Am. Chem. Soc.* **1993**, *115*, 3312–3313.
(67) Eng, M. P.; Albinsson, B. *Angew. Chem., Int. Ed.* **2006**, *45*, 5626–5629.
(68) de la Torre, G.; Giacalone, F.; Segura, J. L.; Martin, N.; Guldi, D. M. *Chem.—Eur. J.* **2005**, *11*, 1267–1280.

our oligo-*p*-xylenes from 0.52 Å$^{-1}$ to 0.77 Å$^{-1}$,[33, 76] and for the DNA hairpins $\beta$ varied from 0.71 Å$^{-1}$ to 1.1 Å$^{-1}$.[63,65] Thus, there is experimental evidence that the distance dependence of long-range electron transfer is influenced by the donor-bridge energy gap not only for strongly $\pi$-conjugated molecules that can mediate charge transfer via a hopping mechanism[26,68] but also for less strongly $\pi$-conjugated molecules where charge injection into the bridge is thermodynamically impossible and where only a tunneling mechanism may be active.

Another interesting point that emerges from our study concerns the importance of intercomponent torsion angles for long-range electronic couplings. The role played by the relative donor, bridge, and acceptor orientations has been investigated in numerous theoretical and experimental studies,[69−72] whereby much work has been stimulated by the observation of biological electron transfer between distant redox partners that are oriented to one another at large torsion angles.[73,74] One recent paper on biphenyl-derivative bridged dyads revealed a 6-fold decrease in electronic donor−acceptor coupling $H_{DA}$ upon increase of the biphenyl torsion angle from 37° to 94°,[75] other studies on (substituted and unsubstituted) biphenyl systems report on effects on the same order of magnitude.[71,72] When extrapolating these results to longer (tri-, tetra-, penta-) phenylene bridges, one would therefore expect a more shallow decrease of $H_{DA}$ with increasing bridge length for spacers with small interphenyl torsion angles than for (substituted) bridges with large dihedral angles between adjacent phenyls. In other words, based on just orientation effects, $\beta$-values should be significantly smaller for charge transfer across oligo-*p*-phenylenes than for oligo-*p*-xylene bridges. However, our experimental observation is that $\beta$-values can be just as low or even lower for the substituted bridges (0.52 Å$^{-1}$)[33,76] than for the unsubstituted phenyl spacers (0.46 Å$^{-1}$, 0.67 Å$^{-1}$, 0.65 Å$^{-1}$),[42,44,58] despite the clearly larger equilibrium torsion angles in the oligo-*p*-xylenes.

## Conclusions

The distance dependence of long-range hole tunneling through oligo-*p*-xylene bridges is sensitive to the energetics of the entire donor-bridge-acceptor system. The experimentally observed variation in distance decay parameters from $\beta = 0.52$ Å$^{-1}$ to 0.77 Å$^{-1}$ when changing from a rhenium to a ruthenium hole donor is in accord with the theoretical expectations based on a simple square wave potential energy barrier model. Donor-bridge energy gaps therefore matter not only for achieving molecular wire behavior in strongly $\pi$-conjugated bridges where *hopping* mechanisms are often active but they also influence the efficiency of the *tunneling* mechanism in the poorly $\pi$-conjugated oligo-*p*-xylene bridges.

## Experimental Section

**Synthesis of the Dyads.** The phenothiazine-xylene-iodo intermediates **4**, **9**, **13**, and **16** (Scheme 2) were previously made by us, and synthetic details and physical characterization data for these compounds have been published recently.[33] These precursors were coupled to a bpy ligand using the following procedure: A suspension of iodo compound (2.3 mmol), 5-(tri-*n*-butyltin)-2,2′-bipyridine (2.6 mmol) in *m*-xylene was deoxygenated by bubbling nitrogen gas during 30 min. After addition of $Pd(PPh_3)_4$ (0.05 mmol) catalyst, the suspension was deoxygenated for an additional 10 min prior to heating to 140 °C for 48 h. After cooling to room temperature, the mixture was concentrated under reduced pressure, and the dark brown oily solid was purified by two successive column chromatographies on silica gel (Merck Kieselgel 60): First using a 98% $CH_2Cl_2$/2% $CH_3OH$ (v/v) eluent mixture and second using an 80% pentane/18% ethyl acetate/2% triethylamine mixture. This gave the pure Stille coupling products **6**, **10**, **14**, and **17** in yields that ranged from 53% (Ru-xy$_4$-PTZ) to 67% (Ru-xy$_2$-PTZ).

**PTZ-xy$_1$-bpy Ligand 6.** $^1$H (400 MHz, $CDCl_3$, 25 °C): $\delta$ = 2.23 (s, 3H, C$H_3$), 2.35 (s, 3H, C$H_3$), 6.12 (dd, $J$ = 8.4, 1.2 Hz, 2H$_{PTZ}$), 6.79 (ddd, $J$ = 7.6, 7.6, 1.2 Hz, 2H$_{PTZ}$), 6.85 (ddd, $J$ = 7.6, 7.6, 1.6 Hz, 2H$_{PTZ}$), 6.97 (dd, $J$ = 7.6, 1.6 Hz, 2H$_{PTZ}$), 7.30 (s, 1H$_{xy}$), 7.35 (ddd, $J$ = 7.6, 4.8, 1.2 Hz, H$_{bpy-5'}$), 7.36 (s, 1H$_{xy}$), 7.85 (ddd, $J$ = 8.4, 7.6, 1.6 Hz, H$_{bpy-4'}$), 7.88 (dd, $J$ = 8.4, 2.4 Hz, H$_{bpy-4}$), 8.47 (ddd, $J$ = 8.0, 1.2, 0.8 Hz, H$_{bpy-3'}$), 8.50 (dd, $J$ = 8.4, 0.8 Hz, H$_{bpy-3}$), 8.73 (ddd, $J$ = 4.8, 1.6, 0.8 Hz, H$_{bpy-6'}$), 8.76 (dd, $J$ = 2.4, 0.8 Hz, H$_{bpy-6}$).

**PTZ-xy$_2$-bpy Ligand 10.** $^1$H (400 MHz, $CDCl_3$, 25 °C): $\delta$ = 2.16 (s, 3H, C$H_3$), 2.18 (s, 3H, C$H_3$), 2.20 (s, 3H, C$H_3$), 2.36 (s, 3H, C$H_3$), 6.11 (dd, $J$ = 8.4, 1.2 Hz, 2H$_{PTZ}$), 6.79 (ddd, $J$ = 7.6, 7.6, 1.2 Hz, 2H$_{PTZ}$), 6.85 (ddd, $J$ = 7.6, 7.6, 1.6 Hz, 2H$_{PTZ}$), 6.97 (dd, $J$ = 7.6, 1.6 Hz, 2H$_{PTZ}$), 7.17 (s, 1H$_{xy}$), 7.23 (s, 1H$_{xy}$), 7.24 (s, 1H$_{xy}$), 7.25 (s, 1H$_{xy}$), 7.37 (ddd, $J$ = 7.6, 4.8, 1.2 Hz, H$_{bpy-5'}$), 7.89 (ddd, $J$ = 8.4, 7.6, 1.6 Hz, H$_{bpy-4'}$), 7.91(dd, $J$ = 8.4, 2.4 Hz, H$_{bpy-4}$), 8.50 (ddd, $J$ = 8.0, 1.2, 0.8 Hz, H$_{bpy-3'}$), 8.52 (dd, $J$ = 8.4, 0.8 Hz, H$_{bpy-3}$), 8.73 (ddd, $J$ = 4.8, 1.6, 0.8 Hz, H$_{bpy-6'}$), 8.77 (dd, $J$ = 2.4, 0.8 Hz, H$_{bpy-6}$).

**PTZ-xy$_3$-bpy Ligand 14.** $^1$H (400 MHz, $CDCl_3$, 25 °C): $\delta$ = 2.15 (s, 9H, C$H_3$), 2.17 (s, 3H, C$H_3$), 2.20 (m, 3H, C$H_3$), 2.35 (s, 3H, C$H_3$), 6.12 (dd, $J$ = 8.4, 1.2 Hz, 2H$_{PTZ}$), 6.79 (ddd, $J$ = 7.6, 7.6, 1.2 Hz, 2H$_{PTZ}$), 6.85 (ddd, $J$ = 7.6, 7.6, 1.6 Hz, 2H$_{PTZ}$), 6.97 (dd, $J$ = 7.6, 1.6 Hz, 2H$_{PTZ}$), 7.09 (d, $J$ = 4.8 Hz, 1H$_{xy}$), 7.11 (d, $J$ = 4.8 Hz, 1H$_{xy}$), 7.17 (d, $J$ = 2.4 Hz, 1H$_{xy}$), 7.22 (s, 1H$_{xy}$), 7.24 (s, 1H$_{xy}$), 7.27 (d, $J$ = 2.4 Hz, 1H$_{xy}$), 7.34 (ddd, $J$ = 7.6, 4.8, 1.2 Hz, H$_{bpy-5'}$), 7.88 (ddd, $J$ = 8.4, 7.6, 1.6 Hz, H $_{bpy-4'}$), 7.93 (dd, $J$ = 8.4, 2.4 Hz, H$_{bpy-4}$), 8.50 (ddd, $J$ = 8.0, 1.2, 0.8 Hz, H$_{bpy-3'}$), 8.52 (dd, $J$ = 8.4, 0.8 Hz, H$_3$), 8.74 (ddd, $J$ = 4.8, 1.6, 0.8 Hz, H$_{bpy-6'}$), 8.78 (dd, $J$ = 2.4, 0.8 Hz, H$_{bpy-6}$).

**PTZ-xy$_4$-bpy Ligand 17.** $^1$H (400 MHz, $CDCl_3$, 25 °C): $\delta$ = 2.17 (m, 18H, C$H_3$), 2.21 (s, 3H, C$H_3$), 2.35 (s, 3H, C$H_3$), 6.14 (d, $J$ = 8.4 Hz, 2H$_{PTZ}$), 6.78 (ddd, $J$ = 7.6, 7.6, 1.2 Hz, 2H$_{PTZ}$), 6.86 (ddd, $J$ = 7.6, 7.6, 1.6 Hz, 2H$_{PTZ}$), 6.97 (dd, $J$ = 7.6, 1.6 Hz, 2H$_{PTZ}$), 7.08 (d, $J$ = 4.8 Hz, 1H$_{xy}$), 7.12 (m, 3H$_{xy}$), 7.18 (d, $J$ = 2.4 Hz, 1H$_{xy}$), 7.23 (s, 1H$_{xy}$), 7.25 (s, 1H$_{xy}$), 7.29 (s, 1H$_{xy}$), 7.35 (ddd, $J$ = 7.6, 4.8, 1.2 Hz, H $_{bpy-5'}$), 7.86 (ddd, $J$ = 8.4, 7.6, 1.6 Hz, H$_{bpy-4'}$),

(69) Larsson, S. *J. Am. Chem. Soc.* **1981**, *103*, 4034–4040.
(70) Cave, R. J.; Siders, P.; Marcus, R. A. *J. Phys. Chem.* **1986**, *90*, 1436–1444.
(71) Helms, A.; Heiler, D.; McLendon, G. *J. Am. Chem. Soc.* **1991**, *113*, 4325–4327.
(72) Benniston, A. C.; Harriman, A.; Li, P. Y.; Sams, C. A.; Ward, M. D. *J. Am. Chem. Soc.* **2004**, *126*, 13630–13631.
(73) Makinen, M. W.; Schichman, S. A.; Hill, S. C.; Gray, H. B. *Science* **1983**, *222*, 929–931.
(74) McGourty, J. L.; Blough, N. V.; Hoffman, B. M. *J. Am. Chem. Soc.* **1983**, *105*, 4470–4472.
(75) Benniston, A. C.; Harriman, A.; Li, P. Y.; Patel, P. V.; Sams, C. A. *Phys. Chem. Chem. Phys.* **2005**, *7*, 3677–3679.
(76) Wenger, O. S. *Coord. Chem. Rev.*[Online early access]. DOI 10.1016/j. ccr.2008.10.010. Published online: **2008**.
(77) Freys, J. C.; Bernardinelli, G.; Wenger, O. S. *Chem. Commun.* **2008**, 4267–4269.

7.91(dd, $J = 8.4$, 2.4 Hz, $H_{bpy\text{-}4}$), 8.48 (ddd, $J = 8.0$, 1.2, 0.8 Hz, $H_{bpy\text{-}3'}$), 8.50 (dd, $J = 8.4$, 0.8 Hz, $H_{bpy\text{-}3}$), 8.74 (ddd, $J = 4.8$, 1.6, 0.8 Hz, $H_{bpy\text{-}6'}$), 8.78 (dd, $J = 2.4$, 0.8 Hz, $H_{bpy\text{-}6}$).

These donor-bridge substituted bipyridine ligands were reacted with the $Ru(bpy)_2Cl_2$ precursor using a 1:1 stoichiometry and a chloroform/ethanol (20%/80%, v/v) solvent mixture.[40] After refluxing under nitrogen atmosphere for 16 h, the orange solution was concentrated under reduced pressure, and the resulting dark solid was purified by two subsequent column chromatographies on the above mentioned silica gel: First using a 98% $CH_2Cl_2$/2% $CH_3OH$ (v/v) eluent mixture and second using a 90% acetonitrile/9% water/1% saturated aqueous $KNO_3$ (v/v/v) eluent mixture. Most of the acetonitrile was evaporated prior to precipitation of the cationic ruthenium(II) target complexes by addition of saturated aqueous $KPF_6$ solution. This procedure resulted in yields around 65% for each of the four Ru-xy$_n$-PTZ molecules from Scheme 1.

**Ru-xy$_1$-PTZ.** $^1$H (400 MHz, $CD_3CN$, 25 °C): $\delta = 1.99$ (s, 3H, C$H_3$), 2.07 (s, 3H, C$H_3$), 6.12 (dd, $J = 8.4$, 1.2 Hz, $2H_{PTZ}$), 6.62 (ddd, $J = 7.6$, 7.6, 1.2 Hz, $2H_{PTZ}$), 6.78 (ddd, $J = 7.6$, 7.6, 1.6 Hz, $2H_{PTZ}$), 6.94 (dd, $J = 7.6$, 1.6 Hz, $2H_{PTZ}$), 6.94 (s, $1H_{xy}$), 7.17 (s, $1H_{xy}$), 7.25 (dd, $J = 7.6$, 7.6 Hz, $1H_{bpy}$), 7.44 (m, $5H_{bpy}$), 7.70 (m, $1H_{bpy}$), 7.78 (m, $4H_{bpy}$), 7.82 (dd, $J = 5.6$, 0.8 Hz, $2H_{bpy}$), 7.91 ($d_{br}$, $J = 5.2$ Hz, $1H_{bpy}$), 8.10 (m, $3H_{bpy}$), 8.58 (m, $3H_{bpy}$), 8.64 (d, $J = 8.0$ Hz, $1H_{bpy}$). MS (ESI): $m/z = 435.6012$ (calcd: 435.6010).

**Ru-xy$_2$-PTZ.** $^1$H (400 MHz, $CD_3CN$, 25 °C): $\delta = 2.04$ (s, 3H, C$H_3$), 2.08 (s, 3H, C$H_3$), 2.11 (s, 3H, C$H_3$), 2.23 (s, 3H, C$H_3$), 6.12 (dd, $J = 8.4$, 1.2 Hz, $2H_{PTZ}$), 6.80 (ddd, $J = 7.6$, 7.6, 1.2 Hz, $2H_{PTZ}$), 6.89 (ddd, $J = 7.6$, 7.6, 1.6 Hz, $2H_{PTZ}$), 6.98 (dd, $J = 7.6$, 1.6 Hz, $2H_{PTZ}$), 7.05 (s, $1H_{xy}$), 7.14 (s, $1H_{xy}$), 7.16 (s, $1H_{xy}$), 7.25 (dd, $J = 7.6$, 7.6 Hz, $1H_{bpy}$), 7.26 (s, $1H_{xy}$), 7.44 (m, $5H_{bpy}$), 7.70 (m, $1H_{bpy}$), 7.78 (m, $4H_{bpy}$), 7.82 (dd, $J = 5.6$, 0.8 Hz, $2H_{bpy}$), 7.91 ($d_{br}$, $J = 5.2$, $1H_{bpy}$), 8.10 (m, $3H_{bpy}$), 8.58 (m, $3H_{bpy}$), 8.64 (d, $J = 8.0$ Hz, $1H_{bpy}$). MS (ESI): $m/z = 487.6302$ (calcd: 487.6323).

**Ru-xy$_3$-PTZ.** $^1$H (400 MHz, $CD_3CN$, 25 °C): $\delta = 2.03$ (s, 3H, C$H_3$), 2.06 (s, 3H, C$H_3$), 2.10 (s, 6H, C$H_3$), 2.24 (s, 3H, C$H_3$), 6.15 (dd, $J = 8.4$, 1.2 Hz, $2H_{PTZ}$), 6.81 (ddd, $J = 7.6$, 7.6, 1.2 Hz, $2H_{PTZ}$), 6.90 (ddd, $J = 7.6$, 7.6, 1.6 Hz, $2H_{PTZ}$), 6.98 (dd, $J = 7.6$, 1.6 Hz, $2H_{PTZ}$), 6.99 (s, $1H_{xy}$), 7.03 (s, $1H_{xy}$), 7.10 (s, $1H_{xy}$), 7.12 (m, $2H_{xy}$), 7.16 (s, $1H_{xy}$), 7.29 (dd, $J = 7.6$, 7.6 Hz, $1H_{bpy}$), 7.40 (m, $5H_{bpy}$), 7.71 (m, $1H_{bpy}$), 7.77 (m, $4H_{bpy}$), 7.82 (dd, $J = 5.6$, 0.8 Hz, $2H_{bpy}$), 7.92 (d, $J = 5.2$ Hz, $1H_{bpy}$), 8.10 (m, $3H_{bpy}$), 8.58 (m, $3H_{bpy}$), 8.64 (d, $J = 8.0$ Hz, $1H_{bpy}$). MS (ESI): $m/z = 539.6658$ (calcd: 539.6636).

**Ru-xy$_4$-PTZ.** $^1$H (400 MHz, $CD_3CN$, 25 °C): $\delta = 2.00$ (s, 3H, C$H_3$), 2.04 (s, 3H, C$H_3$), 2.07 (s, 6H, C$H_3$), 2.10 (s, 3H, C$H_3$), 2.12 (s, 3H, C$H_3$), 2.19 (s, 3H, C$H_3$), 6.11 (dd, $J = 8.4$, 1.2 Hz, $2H_{PTZ}$), 6.79 (ddd, $J = 7.6$, 7.6, 1.2 Hz, $2H_{PTZ}$), 6.90 (ddd, $J = 7.6$, 7.6, 1.6 Hz, $2H_{PTZ}$), 6.98 (dd, $J = 7.6$, 1.6 Hz, $2H_{PTZ}$), 6.99 (s, $1H_{xy}$), 7.03 (s, $1H_{xy}$), 7.09 (s, $1H_{xy}$), 7.11 (m, $4H_{xy}$), 7.17 (s, $1H_{xy}$), 7.30 (dd, $J = 7.6$, 7.6 Hz, $1H_{bpy}$), 7.42 (m, $5H_{bpy}$), 7.70 (m, $1H_{bpy}$), 7.78 (m, $4H_{bpy}$), 7.82 (dd, $J = 5.6$, 0.8 Hz, $2H_{bpy}$), 7.91 (d, $J = 5.2$ Hz, $1H_{bpy}$), 8.10 (m, $3H_{bpy}$), 8.56 (m, $3H_{bpy}$), 8.63 (d, $J = 8.0$ Hz, $1H_{bpy}$). MS (ESI): $m/z = 599.6923$ (calcd: 599.6925).

The NMR, mass spectrometry, optical absorption, and luminescence apparati were the same as in our prior rhenium work.[33,77] The setup for time-resolved luminescence and transient absorption has been described recently.[78]

**Acknowledgment.** This work was supported by the Swiss National Science Foundation, the Société Académique de Genève, and the Fondation Ernest & Lucie Schmidheiny. Professor Andreas Hauser is gratefully acknowledged for letting us use his nanosecond laser setup.

IC801841K

(78) Goze, C.; Leiggener, C.; Liu, S. X.; Sanguinet, L.; Levillain, E.; Hauser, A.; Decurtins, S. *ChemPhysChem.* **2007**, *8*, 1504–1512.